Experimental Analysis and Modelling of Coaxial Transmission Lines with Soft Shield Defects

Hossein Manesh, Abelin Kameni, Florent Loete, Jérôme Genoulaz, Lionel Pichon, Odile Picon

Experimental Analysis and Modelling of Coaxial Transmission Lines with Soft Shield Defects

H. Manesh[1,3], J. Genoulaz[1]
[1] Dept. R&T EWIS Eurasia
Labinal Power Systems (LPS)
Blagnac, France

A. Kameni[2], F. Loete[2], L. Pichon[2]
[2] GeePs (Group of electrical engineering of Paris), CentralSupélec
Université Paris-Sud, UPMC
Gif-sur-Yvette, France

O. Picon[3]
[3] ESYCOM - EA 2552
Université Paris-Est, UPEM
Marne-la-Vallée, France

***Abstract*— Significant research has focused on the diagnosis of "hard" faults (open and short circuits) in transmission lines, but there has been much less work on "soft" faults resulting from a very small change in line impedance. This research is based on one type of soft fault problems in electrical fault diagnosis; the impacts of partial degradation in the coaxial cable shielding or other shielded lines. At first, using classical transmission-line equations in the frequency domain, analytical expressions are derived to infer the impact of the very small discontinuities in transmission lines. Then, this paper illustrates the real experimental measurement cases of faulty shields on coaxial cable. The experimental studies of fault length effects are presented in frequency and time domain measurements by referring to a coaxial cable transmission line designed for high frequency signal transmission in aircraft radio communication systems. Finally, numerical simulation of the experimental case is presented and then validated against the measurement result by using a data processing technique based on time domain analysis.**

Keywords—Fault diagnosis; cable shielding; coaxial cables; frequency-domain reflectometry; soft faults; wire faults; aerospace wiring

I. INTRODUCTION

The fault-detection feature is certainly a very important aspect of wire health monitoring and an important process required in electrical wiring system operation. It has a great influence on the security and quality of supply. In transmission line networks, this feature is needed for the early identification of the faulted line in order to anticipate severe consequences which can be costly and even catastrophic.

Different types of defects can occur on transmission lines. Wire faults can be classified into two main categories depending on their severity [1], [2]: (i) "hard" faults, like short/open circuits, resulting from a significant change in line impedance; and (ii) "soft" faults, which include partial degradation such as insulation damage, natural aging, water infiltration, etc., lead to very small impedance changes along transmission lines.

Significant research has focused on the diagnosis of "hard" faults on transmission lines [3], [4]. These are easier to find because of their significant impact on the resulting signal received by traditional reflectometry measurements. However, the presence of "soft" faults, does not significantly affect the received signal and, in many cases, is undetectable and often masked by background noise. These small faults have been studied less frequently than hard ones and they are more difficult to identify because of their low level signatures until the fault becomes severe [5]-[10].

Soft faults, can seem risk-free and often without significant negative consequences on the system, as they emerge at first. But, a number of factors, including cable aging, inadequate maintenance, hostile environments, etc., can appear, affecting the properties of the wires, after which soft faults can develop into hard faults [11]. Therefore, the soft fault-detection feature in transmission line systems, is needed to provide a timely identification of the faulted line thus anticipating the appearance of severe faults that are initially caused by soft fault degradation.

This research focuses on soft fault problems in electrical fault diagnosis and their weak impact on coaxial transmission lines. The objective of this paper is to carry out a soft fault model in a coaxial line system to analyze its electrical effects caused by discontinuity in the shield. In some cases, this type of discontinuity could have disastrous consequences for the equipment too, as a result of shield effect damage. The faulty part of the cable shield can produce an unwanted reaction on the protective equipment.

This paper aims at investigating the behavior of the line response after shield damage and then to determine fault characteristics from high frequency reflection signals resulting from discontinuities. Reflected signals provide some useful information such as, indicating the health status of the transmission line system and identifying the type of discontinuity and its various effects. In what follows, we examine travelling wave reflection phenomena on transmission lines under faulty shields. Then, from the reflectometry response, we illustrate the reflected signals in time and frequency domains.

The structure of this paper consists of seven sections. Section II shows the characteristics of electromagnetic waves originating from discontinuities in transmission lines. In Section III, the applicability of the reflectometry technique is presented to analyze the faults in time and frequency domains. In Section IV, we use the transmission line equations in the frequency domain and representing the faulty part by means of a local permittivity variation. Analytical expressions are derived to describe the behavior of faults in reflection line response. Section V reports results from faulty shields measured on coaxial cables and discusses a method to eliminate mismatched errors and to remove unwanted reflection. Finally, Section VI illustrates the numerical simulation results for small faults in cable shields. The result is compared with experimental measurements for validation purposes. Section VII provides the conclusion of this work.

II. Electromagnetic Waves Associated with Discontinuities in Transmission Lines

Electromagnetic waves travel along transmission lines of networks and are reflected when they meet a discontinuity along the line or at its extremities. A sudden changing impedance due to the discontinuity on a transmission line leads to the initiation of an electromagnetic wave that is propagated backward from the discontinuity. This phenomenon is characterized by a reflection coefficient whose value depends on the line characteristic impedance and the input impedance of the discontinuity. Line discontinuity can be divided into: junctions with other lines and fault location [12]. Junctions correspond to line extremities connected with more than two lines, that are characterized by a negative reflection coefficient from a junction point in the opposite direction.

The discontinuities caused by a fault can also be classified into two categories, as discussed above. The reflection coefficient of the interruption point where the "hard" fault occurs is close to +1 for open circuits and -1 for short circuits. In "soft" faults, they occur in a portion of the line, as shown in Fig.1. Multiple reflections can occur on the line due to small impedance variations at the interfaces in which the cable sections and faulty area are separated. At each interface of the discontinuity, parts of the signal are reflected and the rest is transmitted. Reflection depends on the severity, the nature and the geometry of the soft fault discontinuity.

Therefore, the domain of the fault location method based on travelling waves is described by a coefficient factor. An observation point can be used at either of the line extremities to measure this factor by reflectometry technique, as explained in more detail in Section III.

III. Application of Reflectometry Methods for Soft Fault Analysis

A. *Reflectometry Method for Testing Cables*

The reflectometry technology has been used over the years in different types of research studies and it is the most promising approach to fault diagnosis in wired networks [7], [13]. It is based on electrical signal injection into the network from one or both extremities of a line followed by an analysis of the reflected signals. By doing so, we are able to study the boundary conditions of the line discontinuity, which can belong to one of the categories discussed in Section II. Subsequently, we can attempt to determine the health status of the line, and indicate the degree of fault severity if the reflections are related to hard and soft fault categories.

Reflectometry techniques can be divided into two broad categories, namely: (i) time-domain reflectometry (TDR) and, (ii) frequency-domain reflectometry (FDR) [13].

The TDR measurement technique launches an impulse or a step into the cable under test and then observes the response in time that can be used to determine the cable status. The position of the discontinuity can be estimated as a function of time providing the cable propagation velocity is known. Discontinuity can also be identified by its response. While the traditional TDR measurement was useful as a qualitative method, it has some limitations that affect its ability and the accuracy of the results [10]: (i) TDR rise time excitation signal against spatial resolution of the measurement and the output frequency range; (ii) low signal reflected ratio against noise.

The FDR measurement technique sends a set of stepped-frequency sine waves down the cable under test, where they are reflected from discontinuities on the cable. This paper focuses on the time and frequency domain analyses generated from the vector network analyzer (VNA) that provides frequency domain response data (S-parameters). The S-parameters data captured using a VNA are defined by transmitted/reflected waves and reflection coefficients.

B. *Impulse Response*

In the reflection mode, a VNA measures the reflection coefficient as a function of frequency. The reflection coefficient can be considered as a relating function of the incident and reflected waves. An inverse transform can convert the reflection coefficient directly to a function of time (the impulse response). It is often needed to obtain the impulse response that allows us to infer the location of the fault and to observe the waveforms initiated by discontinuities along a line.

By means of the inverse Fourier transform, the measurement results are be transformed to time domain

$$y(t) = IFT\left\{U_i(\omega)\cdot\Gamma(\omega)\right\}. \quad (1)$$

where $U_i(\omega)$ is the source signal in frequency domain and $\Gamma(\omega)$ is the reflection function of the FDR.

IV. Analytical Expressions

The aim of this section is to analytically describe the behavior of the reflection line response in the presence of soft faults. We refer to a lossless coaxial cable transmission line of characteristic impedance Z_0.

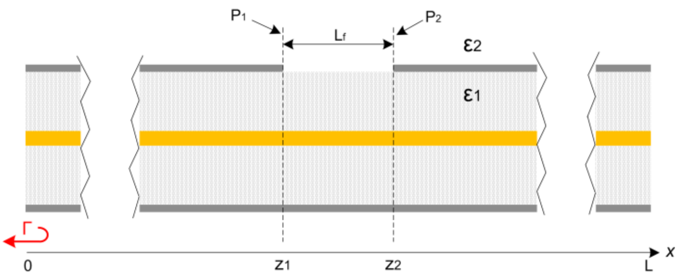

Fig. 1. Illustration of the reflection and transmission boundaries of a coaxial cable with a discontinuity in the shield.

Fig. 1 shows a coaxial transmission line in 2-D with a discontinuity in the shield of length L_f. The model represents the faulty area along the line between two plane interfaces P_1 and P_2, in which the electromagnetic field lines exist partly in the dielectric insulation with ε_1, μ_0, and partly in the surrounding air with ε_2, μ_0, due to the fault in the shield [14].

The resulting transmission-line equations of Fig. 1 are difficult to solve because of the basic assumption of a transverse electromagnetic (TEM) field around the faulty area is not fair and the field distribution over the cross sections is quasi-uniform in this area. Assuming the fault dimension is much lower than the wavelength and the radiation effects are too low, the quasi-TEM analysis can be applied to model the transmission line. Thus, the damaged area between two interfaces at $x = z_1$ and $x = z_2$, are replaced by an equivalent uniform and homogenous transmission line model, wherein the line maintains the same behavior as the original faulty region, and is surrounded by a medium with effective permittivity [15]. This effective value depends on the field confinements in the dielectric insulation and the surrounding air parts on the each side (see Fig.1).

Therefore, we represent a soft fault by means of an effective permittivity change that represents, as a consequence, a shielded damage fault. In addition, in view of very low radiation losses and the lossless line assumption, the line propagation constant is almost imaginary, namely with good approximation: $\gamma = j\beta$, with $\beta = \omega/c$. For the faulty area with constant phase β_f, the effective permittivity can be defined as

$$\varepsilon_{eff}(\omega) = \left(\frac{c \cdot \beta_f(\omega)}{\omega}\right)^2 . \tag{2}$$

Thus, it can be concluded that the effective permittivity must be between the permittivity values on two sides $\epsilon_2 < \epsilon_{eff} < \epsilon_1$.

A common method to analyze this type of problem is to separate the line into a cascade of homogenous and uniform subsections (see Fig. 2). The input reflection coefficient (Γ_{in}) can be determined by the reflectometry response of these cascaded transmission lines.

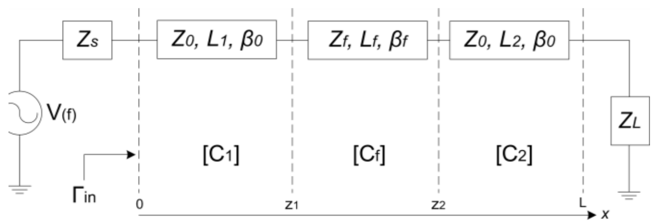

Fig. 2. Sections cascaded transmission line with fault.

In order to analytically simulate line response, the problem is formulated in frequency domain by using the chain transmission line matrix method [16]. The chain matrix of a lossless transmission line can be obtained by characteristic impedance Z_C, phase constant β_0 and the length of the section ℓ, given as

$$[C] = \begin{bmatrix} \cos\beta\ell & jZ_c \sin\beta\ell \\ jY_c \sin\beta\ell & \cos\beta\ell \end{bmatrix} . \tag{3}$$

With $[C_1]$, $[C_F]$ and $[C_2]$ represent the chain parameter matrices for networks in Fig. 2, namely, undamaged for $0 \le x \le z_1$ and $z_2 \le x \le L$, and damaged for $z_1 \le x \le z_2$. The overall chain parameter matrix for the combined circuit is given as

$$[C_T] = [C_1] \cdot [C_F] \cdot [C_2] . \tag{4}$$

The reflection coefficient (Γ_{in}) can be calculated from overall chain parameter matrix of the transmission line sections $[C_T]$.

The boundary conditions at the beginning and the end of the line are represented by means of the source or internal impedance (Z_S) and the load impedance (Z_L). We assumed matched boundary conditions at both line extremities ($Z_S = Z_L = Z_0$), so that there is no re-reflection of the reflected wave from $x = 0$ and $x = L$. Therefore, the reflection coefficient at $x = 0$ represents the one of the overall line under test.

To this end, let us refer to a single transmission line be characterized by a total length $L = 2$ m and let us assume a soft fault occur at $x_f = 0.8$ m from the beginning of the line, with a length $L_f = 2$ cm. The line is characterized by terminal impedances $Z_S = Z_L = Z_0$ and, for the fault, we assume ϵ_{eff} near ϵ_1 : $\epsilon_{eff} = 0.95\ \epsilon_1$ and $\epsilon_{eff} = 0.9\ \epsilon_1$.

From (2) and (4), it is possible to compute the reflection coefficient at $x = 0$ using the chain transmission line matrix method. Fig. 3 shows the reflection coefficient (Γ_{in}) within a frequency spectrum ranging from dc to 2 GHz.

Fig. 4 illustrates time domain reflectometry simulation results $y(t)$ for two aforementioned cases, calculated from (1) where the input signal U_i corresponds to a Gaussian pulse of unit amplitude and $\Gamma(\omega)$ to the reflection function of the FDR at the input of the line.

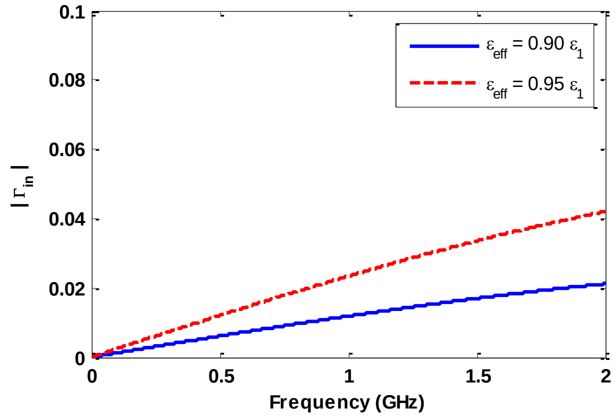

Fig. 3. Reflection coefficient for equivalent transmission lines model at *x=0*.

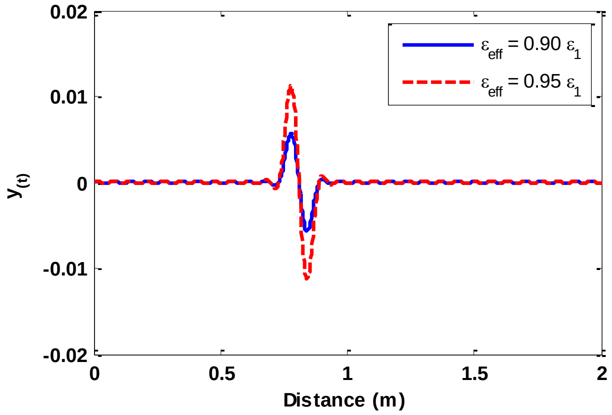

Fig. 4. Signal reflected by the permittivity change proposed model for the faulty transmission line.

As seen in these figures 3 and 4, the amplitude of the reflected waves is generally very small. The time domain result is significantly lower than the incident signal (about 1% of $|U_i|$), as shown in Fig. 4. From Fig. 3, it can further be observed that the amplitude reflected wave in the low frequency range, is lower than 40 dB ($\Gamma < 0.02$), and therefore the reflected pulse cannot be detected easily by means of the measurement devices. As a result, we are interested to work in high frequency ranges.

V. Experimental Measurements

In this section, the experimental measurement that was studied, concerns the small discontinuity in the coaxial cable shield, as presented in Section IV. This can seriously damage the EMI protection provided by the braided-shield cable system. The measurement was carried out by using an aircraft coaxial cable EN 0406-008 WD (Z_0 = 50 ohms) with a single transmission line topology. This type of coaxial cable designed for high frequency radio communication applications in aeronautic environment with frequency operation up to 8GHz. The cable was designed using the new insulation technology, aerated fluoropolymer, namely: a new generation of coaxial cables. The novel assembly technology for aerated fluoropolymer insulation, offers a much faster nominal velocity of propagation, up to 80% of the speed of light c.

As shown in Fig. 5, the fault was made to a section of the shield cutaway of 130°, with a length of 1, 2 and 3 cm. The line terminals were attached with 50 ohms N series RF coaxial cable connectors. These N connectors used to join coaxial cables were designed to carry signals at radio frequencies up to 18 GHz. The reflected signals from the cable under test were measured by means of a Vector Network Analyzer (Rohde & Schwarz ZNB8) operating at a sampling frequency of 100 kHz and 50 ohms input ports impedance. In the case of a measurement with Δf = 100 kHz and a span of 2 GHz, the time domain range could be sufficient to prevent the responses from overlapping or aliasing for reflection measurements [17]. Reflection and transmission coefficients were measured by means of a full 2-port Vector Network Analyzer, with improved TRL calibration for acquiring highly accurate measurements.

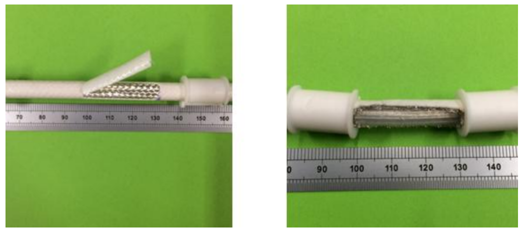

Fig. 5. Shield damage at 8.4 m on a 25 m coaxial cable EN 0406 WD, with different length (i.e., 1, 2, 3 cm).

Fig. 6(a) shows only the experimental measurements of the frequency response $S_{11}(f)$, within a frequency spectrum ranging from 100 kHz to 1 GHz. While Fig. 6(b) illustrates the impulse responses $y(t)$, within a spectrum between 100 kHz to 2 GHz, for a shield soft fault damage with a L_f =3 cm length, located at 8.4 m on a 25 m coaxial cable. As can be observed, these figures also illustrate the results for the same coaxial cable in the undamaged conditions. The frequency-domain reflection results illustrated in Fig. 6(a) are a mix of all the signals reflected by the discontinuities present in the cable over the measured frequency range. As can be seen, in undamaged conditions too, there are ripples in the frequency domain response due to mismatches. It is difficult to estimate the major reflections caused by fault within the cable. However, the time domain results in Fig. 6(b) show the effect of any discontinuities as a function of distance and easily allow to determine the location and magnitude of mismatches from the fault.

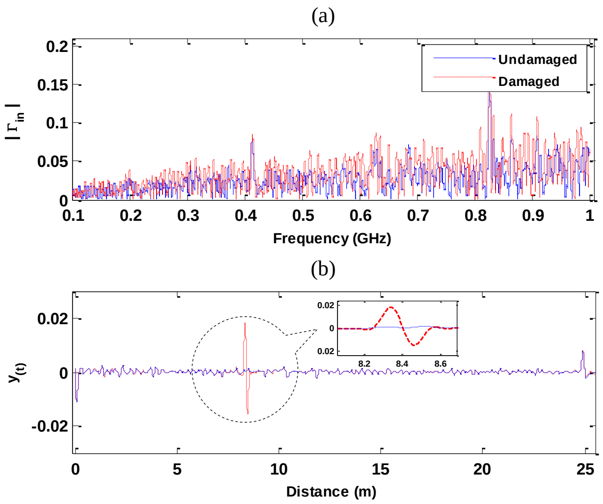

Fig. 6. a) Reflection coefficient amplitudes, b) impulse responses.

Time domain display provides an intuitive way of examining the tested cable characteristics by showing the effect of each discontinuity along the line, as a function of time or distance. The shape of the reflected signals in time domain contains information that is useful in determining the type of the discontinuity, and Fig. 6(b) shows the inductive nature of the discontinuity at x_f = 8.4 m. Indeed, the small discontinuity in the coaxial cables shield, influences the distribution of the external shield current that leads to inductive behavior.

Using both damaged and undamaged results, a time domain filter can be applied to remove unwanted signal components, such as two mismatch effects in Fig.6(b) that produce reflections at the beginning and the end of the cable. The flow-chart shown in Fig. 7, illustrates a step-by-step procedure, in order to compute the reflection coefficient corresponding to the major reflections initiated by the fault.

In the first step, the proposed procedure begins by inverse Fourier transform method (IFT) to compute the time-domain reflected signal from FDR, for the damaged and undamaged cases namely: $S_r(t)$, $S_{ref}(t)$, respectively. The mismatch errors can be eliminated by subtracting the impulse responses $S_r(t)$ from $S_{ref}(t)$. Then, the measured data filtered in the time domain are transformed back to the frequency domain to obtain the reflection coefficient initiated only by fault and without the unwanted signal components (Γ_f).

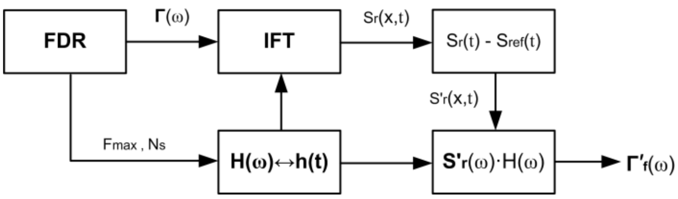

Fig. 7. Flow-chart of the procedure to calculate the shielded fault reflection.

Fig. 8 shows the experimental measurements of the major reflection response initiated by faulty shield on coaxial cable for three lengths of defect, namely, 1, 2, 3 cm, by applying the procedure shown in Fig. 7.

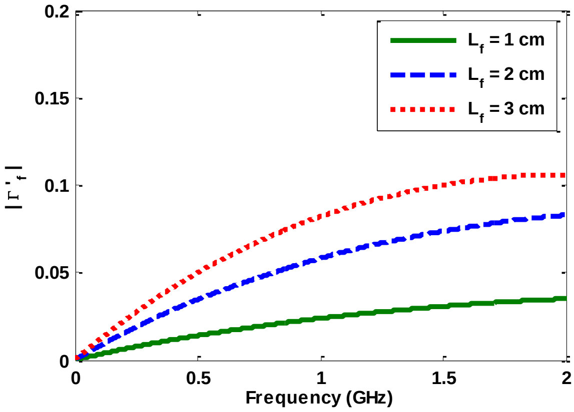

Fig. 8. Reflection coefficients results initiated by shielded damage on coaxial cable.

VI. SIMULATION RESULTS

In this section, we present a numerical validation of the experimental measured results. For this purpose, the application example was applied to the 3-D coaxial cable model. The coaxial line model length was 10 cm and was modeled by means of the constant-parameter model implemented within the CST MICROWAVE STUDIO (CST MWS) simulation environment [18].

Both the cable geometries and the characteristic parameters were inferred from the original reference of the cable example in Section V. The simulation model of the cable is shown in Fig. 9, with dimensions listed in Table I.

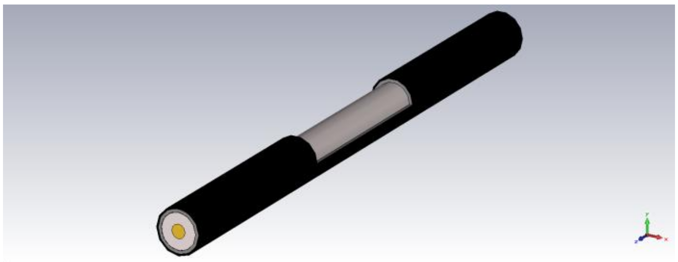

Fig. 9. Coaxial cable model in CST.

TABLE I. COAXIAL CABEL MODEL DEFINITION

Parameter	Material	Diameter (mm)	Electrical Properties
Core	Copper	2.33	σ_c = 5.96 E+7 S/m
Insulation	PTFE (low epsilon)	6.0	ε_r = 1.55
Shield	PEC	7.10	PEC
Jacket	FEP	7.70	2.1

CST MWS offers waveguide port excitation sources to simulate an infinitely long coaxial cable and usually used for S-parameter solution with higher accuracy. Time domain solvers are powerful tools of CST based on solving Maxwell's equations in differential forms. They are remarkably efficient for most HF applications and can calculate the entire broadband frequency response of the simulated system from a single simulation run, when a broadband pulse, such as Gaussian pulse is used as a source.

In this case, part of the field is radiated outside the cable due to a discontinuous shield. The open boundary conditions (PML) are then considered as surrounding the model, in order to emulate an infinite space based on the condition from the experimental measurements. With regard to boundary conditions at the start and end of the modeled cable, they were assumed to be terminated with cable characteristic impedance (matched).

As discussed above, the reflection coefficient initiated by the fault is measured at the beginning of the line placed at 8.4m from the fault position. As already seen in the simulation example, a small section of the cable was used for the simulation. In order to improve the accuracy of the reflection values between the simulation and experimental measurement, we need to specify a unique position for both in which the S-parameters was calculated. By shifting the reference planes of the measurements we could calculate the S-parameters at the simulation reference plane [19]. This new reflection amplitude gave the change in the reflection coefficient on a transmission line due to the presence of losses.

An example of the measured reflection coefficient shifted to the fault position, is shown in Fig. 10 for the test case with the length of 1 and 2 cm defect on shield. Calculations were also done in frequency domain by the numerical simulation test case and they are shown and compared in this figure.

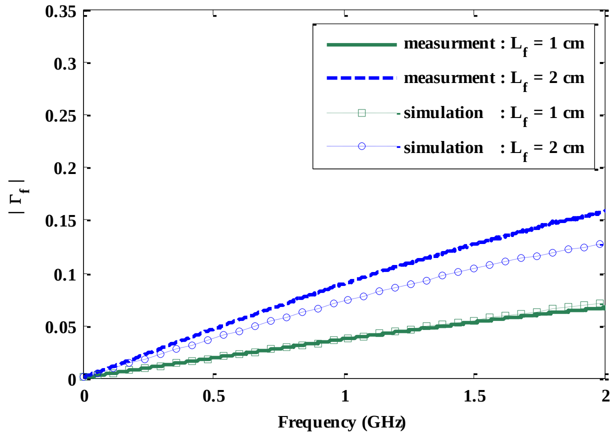

Fig. 10. Measurement and simulation reflection coefficient results of shield damage on coaxial cable.

The reflection coefficients of the fault are shown in Fig.10 as a function of the frequency, between 100 kHz and 2 GHz for two length of defect, namely, 1 and 2 cm. The results show good agreement between simulated and measured values and they are quite satisfactory as they highlight the performance of the simulation model.

VII. Conclusions

In this paper we presented a typical soft fault model on coaxial cable to analyze and estimate the reflection response. Compared to hard faults, these small anomalies do not have significant impacts on the resulting received signal by traditional reflectometry measurements. The reflection results from high frequency electrical signals could provide more useful information to locate the soft fault.

The reflection line response originated by discontinuity in the shield was theoretically demonstrated using analytical expressions in frequency domain, by referring to a lossless coaxial cable transmission line with a local permittivity variation model. The analytical expressions consist of two coaxial lines with different characteristics corresponding to undamaged and damaged line sections. Since the characteristics of the fault section are the unknowns of the problem, we replaced it by an equivalent transmission line model. The analytical demonstration, that have been verified and used for two example cases, is able to approximately characterize the damaged section from the line response calculated by simulation or measurement.

The numerical simulation results are obtained by means of the CST simulation environment, validated by comparison with experimental measurements, and have shown good agreement. Further research is underway to model the shield fault in terms of the distributed transmission line parameters, from reflectometry responses. A soft fault could result in variation of RLCG parameters along the transmission line. By extracting the equivalent circuits for the damaged cable section, the accuracy of analysis for reflections initiated by small faults could also be compared with the experimental measurements.

References

[1] Griffiths, L.A.; Parakh, R.; Furse, C.; Baker, B., "The invisible fray: a critical analysis of the use of reflectometry for fray location," Sensors Journal, IEEE , vol.6, no.3, pp.697,706, June 2006.

[2] Smail, M.K.; Pichon, L.; Olivas, M.; Auzanneau, F.; Lambert, M., "Detection of Defects in Wiring Networks Using Time Domain Reflectometry," Magnetics, IEEE Transactions on , vol.46, no.8, pp.2998,3001, Aug. 2010.

[3] F. Auzanneau, M. Olivas, and N.Ravot, “A simple and accurate model for wire diagnosis using reflectometry,” in PIERS Proc., Aug. 2007.

[4] P. Smith, C. Furse, and J. Gunther, “Analysis of spread spectrum time domain reflectometry for wire fault location,” IEEE Sensors J., vol. 5, pp. 1469–1478, Dec. 2005.

[5] Cerri, G.; De Leo, R.; Della Nebbia, L.; Pennesi, S.; Primiani, V.M.; Russo, P., "Fault location on shielded cables: Electromagnetic modelling and improved measurement data processing," Science, Measurement and Technology, IEE Proceedings, vol.152, no.5, pp.217,226, 9 Sept. 2005.

[6] L. Abboud, A. Cozza, and L. Pichon, “A matched-pulse approach for soft-fault detection in complex wire networks,” IEEE Trans. Instrum. Meas., vol. 61, no. 6, pp. 1719–1732, Jun. 2012.

[7] Tsai, C. Lo, Y. C. Chung, and C. Furse, “Mixed-signal reflectometer for location of faults on aging wiring,” Sensors Journal, IEEE, vol. 5, no. 6, pp. 1479–1482, December 2005.

[8] Qinghua Zhang; Sorine, M.; Admane, M., "Inverse Scattering for Soft Fault Diagnosis in Electric Transmission Lines," Antennas and Propagation, IEEE Transactions on , vol.59, no.1, pp.141,148, Jan. 2011.

[9] Lundquist, E.J.; Nagel, J.R.; Shang Wu; Jones, B.; Furse, C., "Advanced Forward Methods for Complex Wire Fault Modeling," Sensors Journal, IEEE , vol.13, no.4, pp.1172,1179, April 2013.

[10] Franchet, M.; Ravot, N.; Picon, O., "Soft fault detection in cables using the cluster time-frequency domain reflectometry," Electromagnetic Compatibility Magazine, IEEE , vol.2, no.1, pp.54,69, 1St Quarter 2013.

[11] J. Kurek, P. R. Bernstein, M. Etheridge, G. Lasalle, R. McMahon, J Meiner, N. Turner, M. Walz, and C. Gomez, “Aircraft wiring degradation study,” Jan. 2008.

[12] H. Manesh, G. Lugrin, R. Razzaghi, C. Romero, M. Paolone, F. Rachidi, “A new method to locate faults in power networks based on electromagnetic time reversal”, Proc. of 13th IEEE International Workshop on Signal Processing Advances in Wireless Communications, SPAWC, June 2012.

[13] Furse, C.; You Chung Chung; Dangol, R.; Nielsen, M.; Mabey, G.; Woodward, R., "Frequency-domain reflectometry for on-board testing of aging aircraft wiring," Electromagnetic Compatibility, IEEE Transactions on , vol.45, no.2, pp.306,315, May 2003.

[14] C.R. Paul, “Analysis of MulticonductorTransmission Lines”, John Wiley & Sons, NY, 1994.

[15] T. Rozzi, M. Farina, “Advanced Electromagnetic Analysis of Passive and Active Planar Structures”, IEE Electromagnetic Wave Series, vol. 46, Institution of Electrical Engineers, London, 1999.

[16] F.M. Tesche, M. Ianoz, T. Karlsson, “EMC Analysis Methods and Computational Models”, Wiley Int., NY, 1997.

[17] Agilent Technologies, “Time domain analysis using a network analyzer”, Agilent Application Note, 1287-12, 2007.

[18] Computer Simulation Technology Inc (2008). Complete Technology for 3D EM Simulation, [online]. Available: http://www.cst.com

[19] D. M. Pozar, Microwave Engineering. New York: Wesley, 2005.